43rd IEEE Conference on Decision and Control
December 14-17, 2004
Atlantis, Paradise Island, Bahamas

Speed Sensorless Linear Parameter Variant H_∞ Control of the Induction Motor

Dénes Fodor *Member, IEEE* and Roland Tóth, *Student Member, IEEE*

Abstract— **The paper shows the design of a robust control structure for the speed sensorless vector control of the IM, based on the mixed sensitivity (MS) linear parameter variant (LPV) H_∞ control theory. The controller makes possible the direct control of the flux and speed of the motor with torque adaptation in noisy environment. The whole control system is tested by intensive simulations and according to the results it shows good dynamic and robust performance. Implementation issues based on a DSP TMS320F243 development platform are also presented.**

I. Introduction

INDUCTION motors (IM) are widely used in the industry due to their simple structure, low cost, and high reliability. Although they are the horsepower of industry, their control is significantly more challenging than of dc motors, because as a dynamical system they have a highly nonlinear nature with parameter disturbances. This is the reason, why IM's are still not rival to their dc cousins in a number of high precision applications. Nowadays, therefore, there is a great interest in developing high performance and robust controllers to make induction drives unbeatable in all fields of applications. Especially, these efforts concentrate on controllers that do not need speed sensors to operate, which greatly reduces costs and maintenance. (For details see [6], [11]).

Motivated by this goal, we show the design steps of a robust controller for speed sensorless operation of IMs. The designed system gives the opportunity of fast control of the speed of the motor and the magnetic field associated with the rotor flux ($\boldsymbol{\Psi}_r = [\Psi_{r\alpha}, \Psi_{r\beta}]^T$). This system also possesses the ability to operate in noisy environment and the online adaptation to the load torque (T_{load}), which is significant for dynamic tasks. The implemented control law is based on the linear parameter variant (LPV) theory of H_∞ control with mixed sensitivity (MS), which has recently appeared in this field [2], [3]. The controller is supported by an I/O linearized reference model and a complex observer synthesized from an extended Kalman filter (EKF) [8], [13] and a H_∞ observer [10], [14]. This structure needs only the measurements of the stator currents, and it shows robustness with respect to electrical parameter uncertainties, system and measurement noises. Moreover, the proposed control law is designed to be easy to tune, that holds the possibility of the online tuning of the performance.

The paper is organized as follows. The LPV model of the induction motor is given in *Section 2* and the theory of MS LPV H_∞ control in *Section 3*. The design steps of the controller are given in *Section 4* and *Section 5* includes the simulated results. The implementation with a digital signal processor (DSP) is presented in *Section 6* and finally the conclusions are given in *Section 7*.

TABLE I
NOMINAL VALUES OF AN INDUCTION MOTOR

Symbol	Quantity	Nominal Value
L_s	lumped stator 3-phase inductance	0.13 H
L_r	lumped rotor 3-p. inductance	0.13 H
L_m	lumped mutual 3-p. inductance	0.12 H
σ	leakage factor	0.15
R_s	stator 3-p. resistance	1.86 Ω
$R_r(t)$	rotor 3-p. resistance	[3Ω, 6Ω]
R_0	R_r at T_0 temperature	3Ω
$\omega(t)$	rotor angular speed	[-85Hz, 100Hz]
$\omega_{rflux}(t)$	rotor flux angular speed	[-50Hz, 50Hz]
$T_{load}(t)$	load torque	[-100Nm, 100Nm]
m	rotor winding weight	4 kg
c	specific heat ct. (Al)	0.21
T_0	nominal temperature	18°
J	moment of inertia	0.21 J/kgK
p	number of pole pairs	3
F	fraction coefficient	0.001
K_k	linear heat convection	3.5

II. LPV Model of the Induction Motor

In case of assuming that every variable is continually distributed inside of the machine and the magnetic properties of the rotor are ideal, than the mathematical model of the squirrel-cage IM can be easily derived, if we introduce phasors to describe the density distribution of the electrical quantities and magnetic fields around the stator and the

Manuscript received March 7, 2004.This work was supported in part by the Hungarian TéT Foundation under the grant RO-13/2002.

D. F. is with University of Veszprém, Department of Automation, 8200 Veszprém, Egyetem u. 10 ., Hungary. (phone: +36- 88-422022 , fax: +36-88-422022; email: fodor@ieee.org).

R. T. is with the Delft Center for Systems and Control (DCSC), Technical University of Delft, Mekelweg 2, 2628 CD Delft, The Netherlands. (phone: +31-38-3126351, fax: 31-15-2786679; email: tothrola@ieee.org).

0-7803-8682-5/04/$20.00 ©2004 IEEE

rotor [7], [12]. Based on the phasor theory, the relationship between the flux density, describing the magnetic field, the stator current ($\boldsymbol{i}_s = [i_{s\alpha}, i_{s\beta}]^T$), and the stator voltage ($\boldsymbol{u}_s = [u_{s\alpha}, u_{s\beta}]^T$) can be realized through 2 differential and 2 algebraic equations where the rotor angular speed (ω) and the uncertainty of the rotor resistance (R_r) introduce nonlinearity into the system. From these equations, system (1) follows. This is called the stator oriented (α, β) model of the IM, without the motion equation.

$$\frac{d}{dt}\begin{bmatrix}\Psi_{r\alpha}\\ \Psi_{r\beta}\\ i_{s\alpha}\\ i_{s\beta}\end{bmatrix}=\begin{bmatrix}a_1 & -\omega & a_2 & 0\\ \omega & a_1 & 0 & a_2\\ a_3 & \omega a_4 & a_5 & 0\\ -\omega a_4 & a_3 & 0 & a_5\end{bmatrix}\cdot\begin{bmatrix}\Psi_{r\alpha}\\ \Psi_{r\beta}\\ i_{s\alpha}\\ i_{s\beta}\end{bmatrix}+\begin{bmatrix}0 & 0\\ 0 & 0\\ b_1 & 0\\ 0 & b_1\end{bmatrix}\cdot\begin{bmatrix}u_{s\alpha}\\ u_{s\beta}\end{bmatrix}, \quad (1)$$

where the parameters are defined as follows: $a_1 = -1 / \tau_r$, $a_2 = L_m / \tau_r$, $a_3 = \tau / (\sigma \cdot \tau_r)$, $a_4 = \tau / \sigma$, $a_5 = -(\lambda\tau_r + \tau_s) / \sigma$, $b_1 = 1 / (\sigma \cdot L_s)$, $\sigma = 1 - (L_m)^2 / (L_s \cdot L_r)$, $\lambda = (L_m)^2 / L_s$, $\tau = L_m / (L_s \cdot L_r)$, $\tau_r = L_r / R_r$, $\tau_s = L_s / R_s$ and their nominal values are given in *Table 1*.

If R_r is approximated with equation (2) based on the theory of heating materials (aluminum) with linear convection (K_k) of heat [15]:

$$\frac{dR_r}{dt}=R_r\cdot\frac{0.86\cdot R_0}{R_{T0}}\cdot\left(i_{e\_eff}\right)^2-K_k\cdot\left(R_r-R_0\right), \quad (2)$$

where $R_{T0} = (245 + T_0) \cdot m \cdot c$, then with the rotor field orientation (RFO) of the phasors [12], the LPV model of the IM is the following:

$$\frac{d}{dt}\boldsymbol{x}=\boldsymbol{A}(\boldsymbol{p})\cdot\boldsymbol{x}+\boldsymbol{B}\cdot\boldsymbol{u}, \quad (3)$$

where

$$\boldsymbol{A}(\boldsymbol{p})=\begin{bmatrix}a_6 p_2 & a_7 p_2 & 0\\ a_8 p_2 & -\left(a_8 p_2 + a_9\right) & p_3\\ a_{10} p_1 & -p_3 & -\left(a_8 p_2 + a_9\right)\end{bmatrix},$$

$$\boldsymbol{x}=\begin{bmatrix}\Psi_{rd}\\ i_{sd}\\ i_{sq}\end{bmatrix},\quad \boldsymbol{u}=\begin{bmatrix}u_{sd}\\ u_{sq}\end{bmatrix},\quad \boldsymbol{B}=\begin{bmatrix}0 & 0\\ b_1 & 0\\ 0 & b_1\end{bmatrix},$$

$a_6 = -1 / L_r$, $a_7 = L_m / L_r$, $a_8 = a_{10} / \sigma$, $a_9 = \tau_s / \sigma$, $a_{10} = -\lambda / \sigma$. It is clear that, system (3) is an input affine representation where only the state matrix **A** is dependent on the

$$\boldsymbol{p} = [p_1(t)\ \ p_2(t)\ \ p_3(t)]^T = [\omega(t)\ \ R_r(t)\ \ \omega_{rflux}(t)]^T, \quad (4)$$

parameters bounded on the polytopic set given in *Table 1*. These parameters are defined as follows: ω of the IM is given by the dynamic motion equation (5) of the rotor.

$$\frac{d\omega}{dt}=\frac{3p^2L_m}{2JL_r}\cdot\left(\Psi_{rd}\cdot i_{sq}\right)-\frac{p}{J}\cdot\left(T_{load}+F\omega\right). \quad (5)$$

R_r is given by (2) and

$$\omega_{rflux}=\omega+\left(L_m R_r i_{sq}\right)/\left(L_r\Psi_{rd}\right). \quad (6)$$

It is important to note that this RFO LPV model of the IM, gives the possibility to independently control the flux with i_{sd} (see (3)) and ω with i_{sq} (see (5)). This principle is the cornerstone of the proposed algorithm.

III. Mixed Sensitivity LPV H$_\infty$ Control

A. The H$_\infty$ Theory

From the germinal works of Zames [5] to the highly improved theories of the MS MIMO controls [9], [14], the H$_\infty$ theory has conquered great portion of today's controller designs with lots of implemented examples [1]-[3]. Let us give a brief outline of this theory:

For a general control structure with system ***P*** such as in *Fig. 1*, we are searching for an optimal, robust, and stabilizing controller ***K*** that minimizes the H$_\infty$ norm of the system:

$$\left\|\boldsymbol{G}(\boldsymbol{P},\boldsymbol{K})\right\|_\infty=\sup_{\|\boldsymbol{w}(t)\|_2\neq 0}\frac{\left\|\boldsymbol{z}(t)\right\|_2}{\left\|\boldsymbol{w}(t)\right\|_2},\ \ t\in\left(0,\infty\right). \quad (7)$$

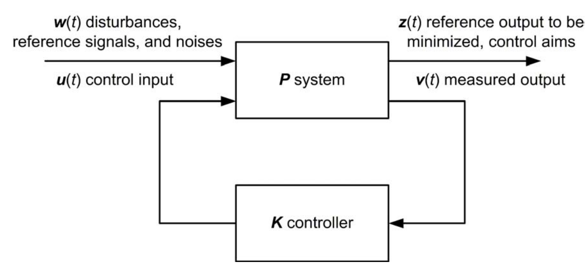

Fig. 1. General problem definition

This optimization is usually solved by a γ-iteration instead of a direct minimization. In each recursive step of this iteration we are looking for a controller that fulfills (8).

$$\left\|\boldsymbol{G}(\boldsymbol{P},\boldsymbol{K})\right\|_\infty<\gamma. \quad (8)$$

In practice, (8) is solved based on the Ricatti equations or linear matrix inequalities (LMIs). The next γ is computed from the pervious step until the solution gets close enough to its optimal value. Moreover, it is proved that this algorithm converges and produces a robust controller which is stable and fulfills (8) on the whole frequency spectrum [9].

B. LPV Systems

The LPV systems are such linear systems, where the $\boldsymbol{A}(.)\ldots\boldsymbol{D}(.)$ matrices in the state-space representation (9), (10) are dependent on a $\boldsymbol{p}(t)$ n dimensional, real parameter

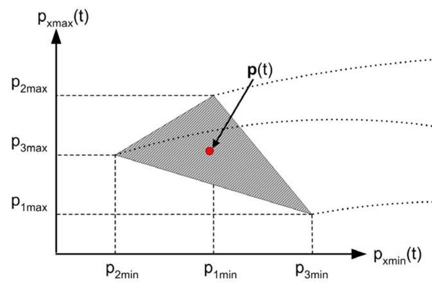

Fig. 2. Polytope form of ***p(t)***

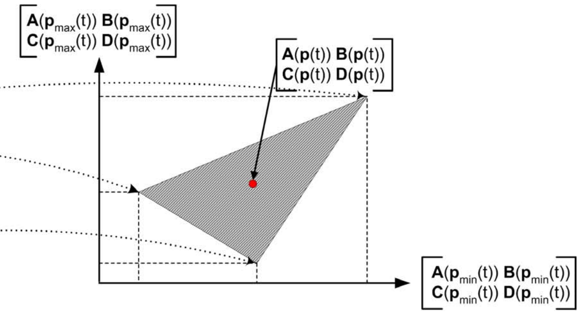

Fig. 3. Polytope of a LPV system dependent on ***p(t)***

vector.

$$\dot{\boldsymbol{x}} = \boldsymbol{A}(\boldsymbol{p})\boldsymbol{x} + \boldsymbol{B}(\boldsymbol{p})\boldsymbol{u} \tag{9}$$

$$\boldsymbol{y} = \boldsymbol{C}(\boldsymbol{p})\boldsymbol{x} + \boldsymbol{D}(\boldsymbol{p})\boldsymbol{u} \tag{10}$$

Further, a LPV system can be imagined as a point by point LTI system moving in an n dimensional system space. Supposing that the system is affine in ***p*** (*Condition #1*), so each of the ***A***(.)…***D***(.) matrices can be transformed into a $\boldsymbol{X}(\boldsymbol{p}) = \boldsymbol{X}_0 + \boldsymbol{X}_1(p_1)+\ldots+\boldsymbol{X}_n(p_n)$ form, and the ***p*** vector is bounded (*Condition #2*), then this system can be described by an n dimensional cube which can be transformed into a polytope (*see Fig. 2 and Fig. 3*) existing on a 2 dimensional system space.

If ***P*** is such an LPV system, than it can be represented by a polytope. For each corner of this polytopic set, such LTI H_∞ controllers can be computed for a given γ, which are the corners of a controller set ***K***. This set is equivalent with a LPV H_∞ controller which fulfills (8). Based on this method, a LPV H_∞ controller can be designed for the LPV model of the IM, because (3) fulfils *Condition #1* and *Condition #2*. In practice, the solution of controller is achieved through LMIs.

C. *Mixed Sensitivity*

By introducing frequency filters (*weighting functions*) on the I/O signals of the system, not only the model of the IM can be more accurately defined, but the properties of the designed controller can be also directly influenced. It can be showed, that the robust stability, disturbance and noise attenuation, and reference tracking of the whole system can be defined, with the frequency definition of the sensitivity function $\boldsymbol{S} = (\boldsymbol{I} + \boldsymbol{GK})^{-1}$, the inverse sensitivity function $\boldsymbol{T} = \boldsymbol{I} - \boldsymbol{S}$, and the closed loop transfer function ***KS***. For a reference tracking objective, the structure presented on *Fig. 4* shall be considered.

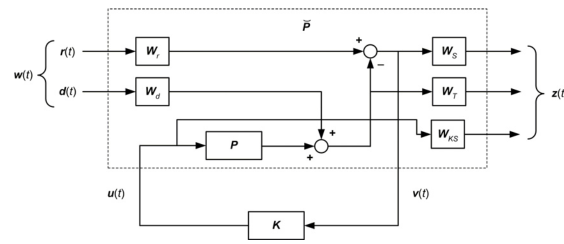

Fig. 4. Mixed sensitivity tracking structure for H_∞ controller design

Here, each of the previously mentioned transfer functions are influenced by the $\boldsymbol{W}_S$, $\boldsymbol{W}_T$, $\boldsymbol{W}_{KS}$ filters, where $\boldsymbol{W}_S$ must be a low-pass filter for good reference tracking, $\boldsymbol{W}_T$ must be a high-pass filter for good noise attenuation, and $\boldsymbol{W}_{KS}$ must be a high-pass filter for robust stability and disturbance attenuation. Moreover, the presented $\boldsymbol{W}_d$ and $\boldsymbol{W}_r$ should be low-pass filters to define the frequency domain of the input signals. If such a structure considered for a H_∞ control objective, then the γ-iteration will find a ***K*** controller that minimizes (11).

$$\left\| \boldsymbol{G}(\boldsymbol{P},\boldsymbol{K}) \right\|_\infty = \left\| \begin{bmatrix} \boldsymbol{W}_S\boldsymbol{S} & \boldsymbol{W}_T\boldsymbol{T} & \boldsymbol{W}_{KS}\boldsymbol{KS} \end{bmatrix}^{\mathrm{T}} \right\|_\infty \tag{11}$$

For an estimation objective by H_∞ observers, in a similar manner, a MS structure is given on *Fig. 5*.

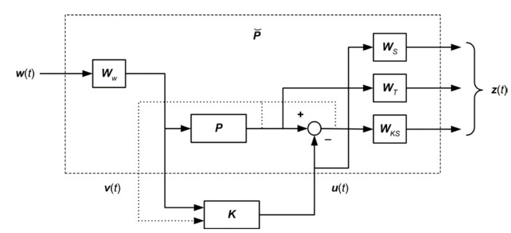

Fig. 5. Mixed sensitivity structure for H_∞ observer design

IV. Speed Sensorless Controller Design

To fulfill the recent requirements for an IM drive control, the controller structure in *Fig. 6* has been proposed. This structure provides the independent control of the speed and flux based only on the measurement of the stator currents. The mechanism is briefly as follows: The measured noisy 3-phase stator currents are transformed to their vectorial representation with the Clark transformation [12], and than they are cleaned from the noise by a complex estimation structure, which is the interconnection of a H_∞ observer and a Kalman filter [8], [13]. Here, the Kalman filter provides the estimation of ω and R_r from the nonlinear equations of the model (2), (5), and the H_∞ observers provides the stator oriented estimation of the rotor flux ($[\Psi_{r\alpha}, \Psi_{r\beta}]^T$), which is needed for the RFO. After RFO, the input reference signals, Ψ_{ref}, ω_{ref} are transformed to current references, $i_{sd(ref)}$ and $i_{sq(ref)}$, by the help of an I/O linearized model of the IM and the previously calculated ω, R_r, Ψ_{rd}, i_{sd}, and i_{sq}. Than, the H_∞ controller gets the deviation $i_{sd(err)}$, $i_{sq(err)}$ from the current reference and calculates the new voltage phasor, which is realized by the Space Vector Pulse Width Modulation (SV PWM) element that directly controls the triggering impulses of the 3 phase inverter generating the desired value of the stator voltage for the IM.

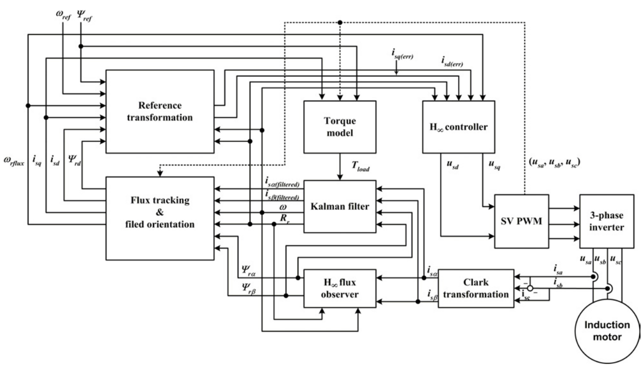

Fig. 6. Speed sensorless control structure

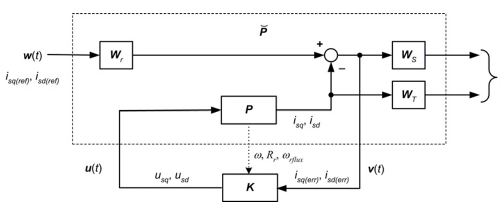

Fig. 7. MS structure for H_∞ tracking

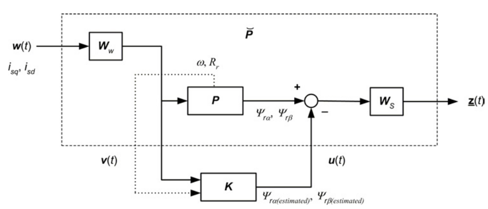

Fig. 8. MS structure for the H_∞ flux observer

The H_∞ controller was designed with the MS structure presented on *Fig. 7*, for the LPV model of the IM (3). This structure inhabits a very rapid control ability of the flux and the speed through the stator current reference. During the design the sensitivity filter $\boldsymbol{W}_S$ was chosen to be

$$\boldsymbol{W}_S(s) = diag(10 / (s + 10), 10 / (s + 10)), \tag{12}$$

providing good reference tracking on low frequency deviations and preventing the controller to be unnecessary aggressive beyond the cutting-off frequency. The amplification of the filter is only 1dB in the passing region, which gives the possibility to tune the speed and accuracy of the control by external amplification of the current reference signals. Because we greatly reduced the uncertainty by the estimation of R_r, there is no need to choose a dynamic filter for $\boldsymbol{W}_T$. By trial and error $\boldsymbol{W}_T$ was designed to be

$$\boldsymbol{W}_T(s) = diag(0.8, 0.8). \tag{13}$$

Furthermore, for $\boldsymbol{W}_r$, the following filter was introduced to restrict the speed of reference tracking which prevents the controller to be unstable even to the step like changes of the reference signals.

$$\boldsymbol{W}_r(s) = diag(15/ (s + 15), 15 / (s + 15)). \tag{14}$$

It has turned out, that almost the half of L_r / R_0 = 43msec for the time constant of (14) provides good tracking without significant overshoots. It is important to note, that because this structure was designed without an integrator an offset error is expected, which is compensated by external gains. However, in opposite to the common practice, this approach also makes possible the external tuning of the controller without destabilizing the whole system.

The optimization was computed through the Matlab function *hinfgs* which is the part of the LMI toolbox. The resulted controller had 5 states, with two inputs and outputs, and it was described with $2^3 = 8$ LTI corner systems, with
$\gamma = 0.6247$. This means, that without external amplification of $i_{sd(err)}$ and $i_{sq(err)}$ the steady state offset error is 62.47%.

The I/O linearization of (3) gives the possibility to transform Ψ_{ref}, ω_{ref} into $i_{sd(ref)}$ and $i_{sq(ref)}$. If the derivatives of Ψ_{rd} and ω are chosen to v_1, v_2 virtual inputs equal to Ψ_{ref}, ω_{ref}, then the following algebraic equation system provides the reference computation:

$$i_{sd(ref)} = L_r v_1 / (L_m R_r) + \Psi_{rd} / L_m, \tag{15}$$
$$i_{sq(ref)} = \tau_{mech} v_1 / (p\Psi_{rd}) + \tau_{mech}(T_{load} + F\omega), \tag{16}$$

where $\tau_{mech} = 2JL_r / 3pL_m$. The (15) and (16) equations can handle the transformation task when $\Psi_{rd} \neq 0$ which only occurs when the system is at zero energy. At this point, any value can be assigned to the flux in equations (15) and (16), because this situation exists only for a very short time, during startup.

The flux orientation is handled through the Park transformation [12], to which the needed flux angle is computed from the real and imaginary part of the estimated flux vector. It is clear that for accurate operation we need a very good estimation of the real flux. This is the main reason, why such a complex structure is used for the estimation task. Even in noisy environment, the H_∞ observers are capable for this very accurate estimation because of their low-pass property. Thus, for the stator oriented LPV flux model of the IM

$$\frac{d}{dt}\begin{bmatrix}\Psi_{r\alpha}\\ \Psi_{r\beta}\end{bmatrix}=\begin{bmatrix}a_6 p_2 & -p_1\\ p_1 & a_6 p_2\end{bmatrix}\cdot\begin{bmatrix}\Psi_{r\alpha}\\ \Psi_{r\beta}\end{bmatrix}+\begin{bmatrix}a_7 p_2 & 0\\ 0 & a_7 p_2\end{bmatrix}\cdot\begin{bmatrix}i_{r\alpha}\\ i_{r\beta}\end{bmatrix}, \quad (17)$$

the MS structure on *Fig. 8* was used to calculate an H_∞ observer with the *hinfgs* function. In this structure the frequency of the nonfiltered deviations was chosen to be greater than 300Hz, so the introduced sensitivity filter was

$$\boldsymbol{W}_S(s) = diag(300 / (s + 30), 300 / (s + 30)). \quad (18)$$

Because any kind of disturbance can shock the system, $\boldsymbol{W}_w$ was omitted for wide interval of functioning. The resulted observer had a $\gamma = 8.49 \cdot 10^{-5}$. Although, this observer calculates the flux vector, the unknown values of ω and R_r are still needed. To obtain them, an EKF is attached to the observer. This EKF based on the (1), (2), (5) nonlinear equations, where $u_{s\alpha}$, $u_{s\beta}$, T_{load} are used as known inputs and $i_{s\alpha}$, $i_{s\beta}$ are used as the measured outputs of the system. Because of the strong dynamical properties of the resulted model, the prediction phase (see [11]) of this EKF is computed trough a 3rd order recursive Adams-Bashforth numerical method [4]. In the correction phase of the EKF only the diagonal elements of $\boldsymbol{Q}$ (expected variance of the system noise) and $\boldsymbol{R}$ (expected variance of the measurement noise) were chosen to be nonzeros. It is not a strict assumption, because there is no significant cross coupling between these noises in the real environment. For this reason: $\boldsymbol{Q}_{ij} = 0$, expect $\boldsymbol{Q}(i_{s\alpha}, i_{s\alpha}) = \boldsymbol{Q}(i_{s\beta}, i_{s\beta}) = 0.0117h / (L_s\sigma)$; $\{0, 1,\ldots, 6\} \ni i,j$ and $\boldsymbol{R}_{kz} = 0$, expect $\boldsymbol{R}(i_{s\alpha}, i_{s\alpha}) = \boldsymbol{R}(i_{s\beta}, i_{s\beta}) = 13.85$, $\boldsymbol{R}(\Psi_{r\alpha}, \Psi_{r\alpha}) = \boldsymbol{R}(\Psi_{r\beta}, \Psi_{r\beta}) = 0.0205$; $\{0, 1,\ldots, 4\} \ni j,z$, where h is the step size of the numerical algorithm.

The estimation also supported by a torque reference model (19), which calculates the expected load torque from the reference signals, weighted by the filter given with (14), and from the measured currents.

$$T_{load} = \tau_{mech}(\Psi_{rd} i_{sq}) - F\omega_{ref}\,. \quad (19)$$

The whole estimation structure was tuned to be perfectly functioning with only 0.5% of prediction error, while heavy measurement noise (*Fig. 9*), inverter noise (*Fig. 10*), and 5% parameter uncertainties was introduced into the Matlab simulations, during the design.

V. Simulation Results

The controller was tested in Matlab with the help of the Simulink model of the IM. During a very dynamic task where the load torque changed as in *Fig. 13*, the reference tracking for speed occurred as in *Fig. 11*, while the rotor flux was changing as in *Fig. 12*. Additionally, *Fig. 14* and *Fig. 15* shows the controller given stator voltages, during this simulation.

By looking to these results, it can be concluded that the controller works well even in rapidly changing load conditions (like at 0.5 msec) and its tracking accuracy and dynamics are good even for large reference steps (like at 3.5 msec). The controller was also tested for robustness. With 5% of parameter variance the maximum tracking error in speed was no more than 6.5%.

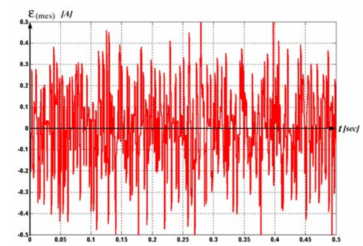

Fig. 9. Modeled measurement noise during design

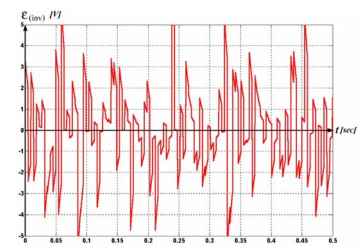

Fig. 10. Modeled inverter noise during design

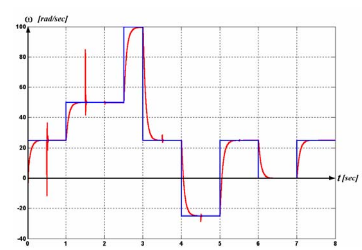

Fig. 11. Reference tracking for ω

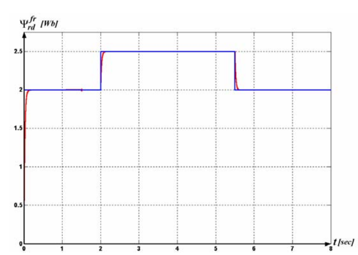

Fig. 12. Reference tracking for Ψ_{rd}

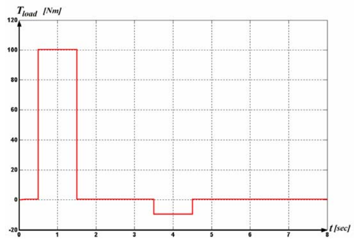

Fig. 13. Change of T_{load}

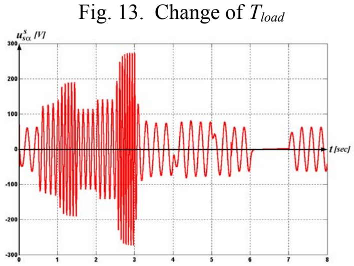

Fig. 14. Change of $u_{s\alpha}$

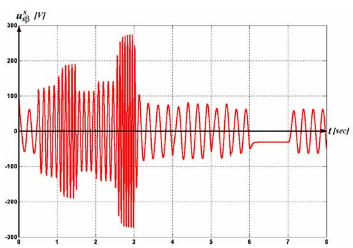

Fig. 15. Change of $u_{s\beta}$

VI. Implementation with TMS320F243

The proposed controller is under implementation on a Digital Spectrum motion control development kit which is powered by a TMS320F243 DSP. This fixed point DSP processor is capable of 20Mips and the processors board contains 8K word Flash ROM. The processor board directly connects to an inverter interface card which produces the PWM signals for a $300V_p$ AC capable inverter that empowers the IM seen on *Table 1*. This interface card also contains analog to digital converters (ADC) which are used to get to know the values of the stator currents and a dedicated Space-Vector-PWM calculator circuit which is responsible to directly give the PWM signals to the inverter. The connection of the structure is presented on *Fig. 16*.

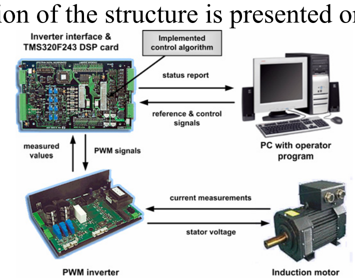

Fig. 16. Implemented AC drive with DSP control

The program of the DSP card is developed in Code Composer. During implementation, the continuous controller system was discretised by the Euler method with a chosen step size of 1msec, considered enough to represent the continuous controller. Even with the drawback of the fixed point calculations the implementation promises acceptable performance. The program running time is actually 57,9msec for a control cycle, which is too long for real time control. We work intensively in code optimization to fulfill the constraints raised by the motor time constant.

VII. Conclusion

In this paper our aim was to show the design steps of a state of the art controller for speed sensorless robust operation of the IM, taking into account the load torque changes without the loss of reference accuracy and effectiveness of the whole drive. It is clearly turned out, that with the use of the MS LPV H_∞ control theory the proposed task can be handled and even implemented on a DSP hardware. However, this structure gives the opportunity of accurate control of the given IM with a parameter variance no more than 5%, its usage would be greatly improved with an online tuning algorithm which is in the focus of our future research.

References

[1] C. H. Lee M. H. Shin and M. J. Chung: "A Design of Gain-Scheduled Control for a Linear Parameter Varying System: An Application to Flight Control," Control Engineering Practice, No. 9, 2001, pp. 11-21.

[2] D. Fodor L. Szalay and K. Bíró: "H_∞ Output Feedback Controller Design for AC Motor Control," in Proceedings of 10th International Power Electronics and Motion Conference, EPE-PEMC, 2002.

[3] E. Premapain I. Pstletwaite and A. Benchaib: "A Linear Parameter Variant H_∞ Control Design for an Induction Motor," Control Engineering Practice, No. 10, 2002, pp. 663-644.

[4] F. Hartung: Introduction to Numerical Analysis, in Hungarian, University of Veszprém, Veszprém: 1998, pp 336-340.

[5] G. Zames: "Feedback and Optimal Sensitivity: Model Reference Transformations, Multiplicative Seminorms and Approximate Inverse," IEEE Transactions on Automatic Control, Vol. 26, No. 1, 1981, pp. 301-320.

[6] J. Holtz: "Sensorless Control of Induction Drives," in Proceedings of the IEEE, Vol. 90, No. 8, 2002, pp. 1259-1394.

[7] J. Holtz: "The Representation of AC Machine Dynamics by Complex Signal Flow Graphs," IEEE Transactions on Industrial Electronics, Vol. 42, No. 3, 1995, pp. 263-271.

[8] K. J. Åström and B. Wittenmark: Computer Controlled Systems, Prentice-Hall, New York: 1990, pp 350-356.

[9] K. Zhou and J. C. Doyle: *Essentials of Robust Control*, Prentice-Hall, New York: 1998, pp 269-300, 315-342.

[10] M. Hilairet C. Darengosse F. Auger and P. Chevrel: "Synthesis and Analysis of Robust Flux Observers for Induction Machines," Bd. de l'Université, France: 2000.

[11] P. Vas: Sensorless *Vector and Direct Torque Control*, Oxford University Press, Oxford: 1998, pp. 1-86, 263-304.

[12] P.K. Kovács: *Transient Phenomena in Electrical Machines*, Akadémiai kiadó, Budapest: 1954, pp 13-41.

[13] R. E. Kálmán: "A New Approach to Linear Filtering and Prediction Problem," Journal Basic Engineering, Vol. 82, 1960, pp. 34-45.

[14] S. Skogestad and I. Postlethwaite: *Multivariable Feedback Control*, John Wiley & Sons, Chichester: 1996, pp 362-396.

[15] V. Uray: *Elektrotechnics*, in Hungarian, Műszaki könyvkiadó, Budapest: 1970, pp. 82-84.